Aaij, R. et al. (2013) Measurement of the fragmentation fraction ratio fs/fd and its dependence on B meson kinematics. Journal of High Energy Physics, 2013 (1). ISSN 1029-8479

http://eprints.gla.ac.uk/82358/

Deposited on: 9 July 2013

Measurement of the fragmentation fraction ratio f_s/f_d and its dependence on B meson kinematics

The LHCb collaboration

E-mail: Barbara.Storaci@cern.ch

ABSTRACT: The relative production rate of B_s^0 and B^0 mesons is determined with the hadronic decays $B_s^0 \to D_s^- \pi^+$ and $B^0 \to D^- K^+$. The measurement uses data corresponding to $1.0\,\text{fb}^{-1}$ of pp collisions at a centre-of-mass energy of $\sqrt{s} = 7\,\text{TeV}$ recorded in the forward region with the LHCb experiment. The ratio of production rates, f_s/f_d, is measured to be $0.238 \pm 0.004 \pm 0.015 \pm 0.021$, where the first uncertainty is statistical, the second systematic, and the third theoretical. This is combined with a previous LHCb measurement to obtain $f_s/f_d = 0.256 \pm 0.020$. The dependence of f_s/f_d on the transverse momentum and pseudorapidity of the B meson is determined using the decays $B_s^0 \to D_s^- \pi^+$ and $B^0 \to D^- \pi^+$. There is evidence for a decrease with increasing transverse momentum, whereas the ratio remains constant as a function of pseudorapidity. In addition, the ratio of branching fractions of the decays $B^0 \to D^- K^+$ and $B^0 \to D^- \pi^+$ is measured to be $0.0822 \pm 0.0011\,(\text{stat}) \pm 0.0025\,(\text{syst})$.

Contents

1 Introduction

The ratio of fragmentation fractions f_s/f_d quantifies the relative production rate of B_s^0 mesons with respect to B^0 mesons. Knowledge of this quantity is essential when determining any B_s^0 branching fraction at the LHC. The measurement of the branching fraction of the rare decay $B_s^0 \to \mu^+\mu^-$ [1] is the prime example where a precise measurement of f_s/f_d is crucial for reaching the highest sensitivity in the search for physics beyond the Standard Model. The branching fractions of a large number of B^0 and B^+ decays have been measured to high precision at the B factories [2], but no B_s^0 branching fraction is yet known with sufficiently high precision to be used as a normalisation channel.

The relative production rates of b hadrons are determined by the fragmentation fractions f_u, f_d, f_s, f_c and f_Λ, which describe the probability that a b quark will hadronize into a B_q meson (where $q = u, d, s, c$), or a b baryon, respectively[1]. The ratio of fragmentation fractions f_s/f_d has been previously measured at LHCb with hadronic [3] and semileptonic decays [4], and the resulting values were combined [4].

In this paper, the ratio of fragmentation fractions f_s/f_d is determined using $B_s^0 \to D_s^-\pi^+$ and $B^0 \to D^-K^+$ decays collected in pp collisions at a centre-of-mass energy of $\sqrt{s} = 7\,\text{TeV}$, with data corresponding to an integrated luminosity of 1.0 fb^{-1} recorded with the LHCb detector. Since the framework of factorization is well applicable to these decays [5], their ratio of branching fractions is theoretically well understood [6] and their

---

[1]Charge conjugation is implied throughout this paper.

relative decay rates can be used to determine the ratio of fragmentation fractions for B_s^0 and B^0 mesons through

$$\frac{f_s}{f_d} = \frac{\mathcal{B}(B^0 \to D^- K^+)}{\mathcal{B}(B_s^0 \to D_s^- \pi^+)} \frac{\epsilon_{DK}}{\epsilon_{D_s\pi}} \frac{N_{D_s\pi}}{N_{DK}}$$

$$= \Phi_{\mathrm{PS}} \left|\frac{V_{us}}{V_{ud}}\right|^2 \left(\frac{f_K}{f_\pi}\right)^2 \frac{\tau_{B^0}}{\tau_{B_s^0}} \frac{1}{\mathcal{N}_a \mathcal{N}_F} \frac{\mathcal{B}(D^- \to K^+ \pi^- \pi^-)}{\mathcal{B}(D_s^- \to K^+ K^- \pi^-)} \frac{\epsilon_{DK}}{\epsilon_{D_s\pi}} \frac{N_{D_s\pi}}{N_{DK}}, \qquad (1.1)$$

where N corresponds to a signal yield, ϵ corresponds to a total efficiency, $\tau_{B_s^0}/\tau_{B^0} = 0.984 \pm 0.011$ [7] corresponds to the ratio of lifetimes and $\mathcal{B}(D^- \to K^+ \pi^- \pi^-) = (9.14 \pm 0.20)\%$ [8] and $\mathcal{B}(D_s^- \to K^+ K^- \pi^-) = (5.50 \pm 0.27)\%$ [9] correspond to the $D_{(s)}^-$ meson branching fractions. The factor $\mathcal{N}_a = 1.00 \pm 0.02$ accounts for the ratio of non-factorizable corrections [10], $\mathcal{N}_F = 1.092 \pm 0.093$ for the ratio of $B_{(s)}^0 \to D_{(s)}^-$ form factors [11], and $\Phi_{\mathrm{PS}} = 0.971$ for the difference in phase space due to the mass differences of the initial and final state particles. The numerical values used for the CKM matrix elements are $|V_{us}| = 0.2252$, $|V_{ud}| = 0.97425$, and for the decay constants are $f_\pi = 130.41\,\mathrm{MeV}$, $f_K = 156.1\,\mathrm{MeV}$, with negligible uncertainties, below 1% [2]. The measurement is not statistically limited by the size of the $B^0 \to D^- K^+$ sample , and therefore the theoretically less clean $B^0 \to D^- \pi^+$ decays, where exchange diagrams contribute to the total amplitude, do not contribute to the knowledge of f_s/f_d .

The ratio of fragmentation fractions can depend on the centre-of-mass energy, as well as on the kinematics of the $B_{(s)}^0$ meson, as was studied previously at LHCb with partially reconstructed B decays [4]. The dependence of the ratio of fragmentation fractions on the transverse momentum p_{T} and pseudorapidity η of the $B_{(s)}^0$ meson is determined using fully reconstructed $B^0 \to D^- \pi^+$ and $B_s^0 \to D_s^- \pi^+$ decays. Since it is only the dependence that is of interest here, the more abundant $B^0 \to D^- \pi^+$ decay is used rather than the $B^0 \to D^- K^+$ decay. The $B^0 \to D^- K^+$ and $B^0 \to D^- \pi^+$ decays are also used to determine their ratio of branching fractions, which can be used to quantify non-factorizable effects in such heavy-to-light decays [10].

The paper is organised as follows: the detector is described in section 2, followed by the event selection and the relative selection efficiencies in section 3. The fit to the mass distributions and the determination of the signal yields are discussed in section 4. The systematic uncertainties are presented in section 5, and the final results are given in section 6.

2 Detector and software

The LHCb detector [12] is a single-arm forward spectrometer covering the pseudorapidity range $2 < \eta < 5$, designed for the study of particles containing b or c quarks. The detector includes a high precision tracking system consisting of a silicon-strip vertex detector surrounding the pp interaction region, a large-area silicon-strip detector located upstream of a dipole magnet with a bending power of about $4\,\mathrm{Tm}$, and three stations of silicon-strip detectors and straw drift tubes placed downstream. Data are taken with both magnet polarities. The combined tracking system has momentum resolution $\Delta p/p$ that varies from

0.4% at $5\,\mathrm{GeV}/c$ to 0.6% at $100\,\mathrm{GeV}/c$, and impact parameter[2] resolution of $20\,\mathrm{\mu m}$ for tracks with high transverse momentum. Charged hadrons are identified using two ring-imaging Cherenkov detectors.

The trigger [13] consists of a hardware stage, based on information from the calorimeter and muon systems, followed by a software stage which applies a full event reconstruction. The events used in this analysis are selected at the hardware stage by requiring a cluster in the calorimeters with transverse energy larger than $3.6\,\mathrm{GeV}$. The software stage requires a two-, three- or four-track secondary vertex with a high sum of the p_{T} of the tracks and a significant displacement from the primary pp interaction vertices (PVs). At least one track should have p_{T} greater than $1.7\,\mathrm{GeV}/c$, track fit χ^2 over the number of degrees of freedom less than two, and IP χ^2 with respect to the associated primary interaction greater than sixteen. The IP χ^2 is defined as the difference between the χ^2 from the vertex fit of the associated PV reconstructed with and without the considered track. A multivariate algorithm is used for the identification of the secondary vertices consistent with the decay of a b hadron.

In the simulation, pp collisions are generated using PYTHIA 6.4 [14] with a specific LHCb configuration [15]. Decays of hadronic particles are described by EvtGen [16], whilst final state radiation is generated using PHOTOS [17]. The interaction of the generated particles with the detector and its response are implemented using the GEANT4 toolkit [18, 19] as described in ref. [20].

3 Event selection

The three decay modes, $B^0 \to D^- \pi^+$, $B^0 \to D^- K^+$ and $B_s^0 \to D_s^- \pi^+$, are topologically very similar and can therefore be selected using the same event selection criteria, thus minimizing efficiency differences between the modes. The $B_{(s)}^0$ candidates are reconstructed from a $D_{(s)}^-$ candidate and an additional pion or kaon (the "bachelor" particle), with the $D_{(s)}^-$ meson decaying to $K^+ \pi^- \pi^-$ ($K^+ K^- \pi^-$).

After the trigger selection, a loose preselection is made using the $B_{(s)}^0$ and $D_{(s)}^-$ masses, lifetimes and vertex qualities. A boosted decision tree (BDT) [21] is used to further separate signal from background. The BDT is trained on half the $B_s^0 \to D_s^- \pi^+$ data sample. The most discriminating variables are the $B_{(s)}^0$ impact parameter χ^2, the pointing angle of the $B_{(s)}^0$ candidate to the primary vertex and the p_{T} of the tracks. A cut value for the BDT output variable was chosen to optimally reduce the number of combinatorial background events, retaining approximately 84% of the signal events.

The $D_{(s)}^-$ candidates are identified by requiring the invariant mass under the $K^+ \pi^- \pi^-$ ($K^+ K^- \pi^-$) hypothesis to fall within the selection window 1844–1890 (1944–1990) MeV/c^2. The relative efficiency of the selection procedure is evaluated for all decay modes using simulated events, generated with the appropriate Dalitz plot structures [22, 23]. Since the analysis is only sensitive to relative efficiencies, the impact of any discrepancy between data and simulation is small.

---

[2]Impact parameter (IP) is defined as the transverse distance of closest approach between the track and a primary interaction.

The final $B_s^0 \to D_s^- \pi^+$, $B^0 \to D^- \pi^+$ and $B^0 \to D^- K^+$ event samples are obtained after particle identification (PID) criteria, based on the difference in log-likelihood between the kaon and pion hypotheses (DLL). The PID performance as a function of $p_{\rm T}$ and η of the track is estimated from data using a calibration sample of approximately 27 million $D^{*-} \to \overline{D}^0(K^+\pi^-)\pi^-$ decays, which are selected using kinematic criteria only. A cut on the bachelor particle is placed at DLL$(K-\pi)< 0$ to select the $B_s^0 \to D_s^- \pi^+$ and $B^0 \to D^- \pi^+$ event samples and at DLL$(K-\pi)> 5$ to select the $B^0 \to D^- K^+$ sample. These requirements have an average efficiency of 85.5% and 73.0% respectively with a misidentification probability of 8.81% and 2.77%. The $D_s^- \to K^+ K^- \pi^-$ decay is further distinguished from $D^- \to K^+ \pi^- \pi^-$ decays by imposing DLL$(K-\pi)> 5$ on the kaon candidate with the same charge as the D meson, whilst the DLL criteria for the π^- and K^+ are identical between D^- and D_s^- and are used to discriminate $D_{(s)}^-$ decays from background. The total (PID and invariant mass) efficiency to select the D^- (D_s^-) particle is 84.6% (78.5%) with a misidentification probability of 4.57% (0.77%).

4   Event yields

The relative yields of the three decay modes are determined from unbinned extended maximum likelihood fits to the mass distributions of the reconstructed $B_{(s)}^0$ candidates as shown in figure 1. In order to achieve the highest sensitivity, the sample is separated according to the two magnet polarities, allowing for possible differences in PID performance and in running conditions. A simultaneous fit to the two magnet polarities is performed for each decay mode, with the peak position and width of each signal shared between the two.

The signal mass shape is described by a Gaussian distribution with power-law tails on either side to model the radiative tail and non-Gaussian detector effects. It consists of a Crystal Ball function [24]

$$
f_{\rm left}(m, \alpha, n, \mu, \sigma) = N \cdot \begin{cases} e^{-\frac{(m-\mu)^2}{2\sigma^2}}, & \text{for } \dfrac{m-\mu}{\sigma} > -\alpha \\ \left(\dfrac{n}{|\alpha|}\right)^n \cdot e^{-|\alpha|^2/2} \cdot \left(\dfrac{n}{|\alpha|} - |\alpha| - \dfrac{m-\mu}{\sigma}\right)^{-n}, & \text{for } \dfrac{m-\mu}{\sigma} \leq -\alpha \end{cases}
$$

(4.1)

and a second, similar but mirrored, function to describe the right tail, resulting in the signal mass shape $f_{\rm 2CB}(m) = f_{\rm left}(m) + f_{\rm right}(m)$. The parameters of the tails are obtained from simulated events. The mean μ and the width σ of the Gaussian distribution are equal in both Crystal Ball functions, and are allowed to vary in the fit. The parameter N is a normalisation factor.

Three classes of background are considered in the fit: fully reconstructed decays where at least one track is misidentified, partially reconstructed decays with or without misidentified tracks and combinatorial background. The shapes of the invariant mass distributions for the partially reconstructed decays are taken from large samples of simulated events. The main sources are $B^0 \to D^- \rho^+$ and $B^0 \to D^{*-} \pi^+(K^+)$ for the $B^0 \to D^- \pi^+(K^+)$ sample, and $B_s^0 \to D_s^- \rho^+$ and $B_s^0 \to D_s^{*-} \pi^+$ for the $B_s^0 \to D_s^- \pi^+$ sample.
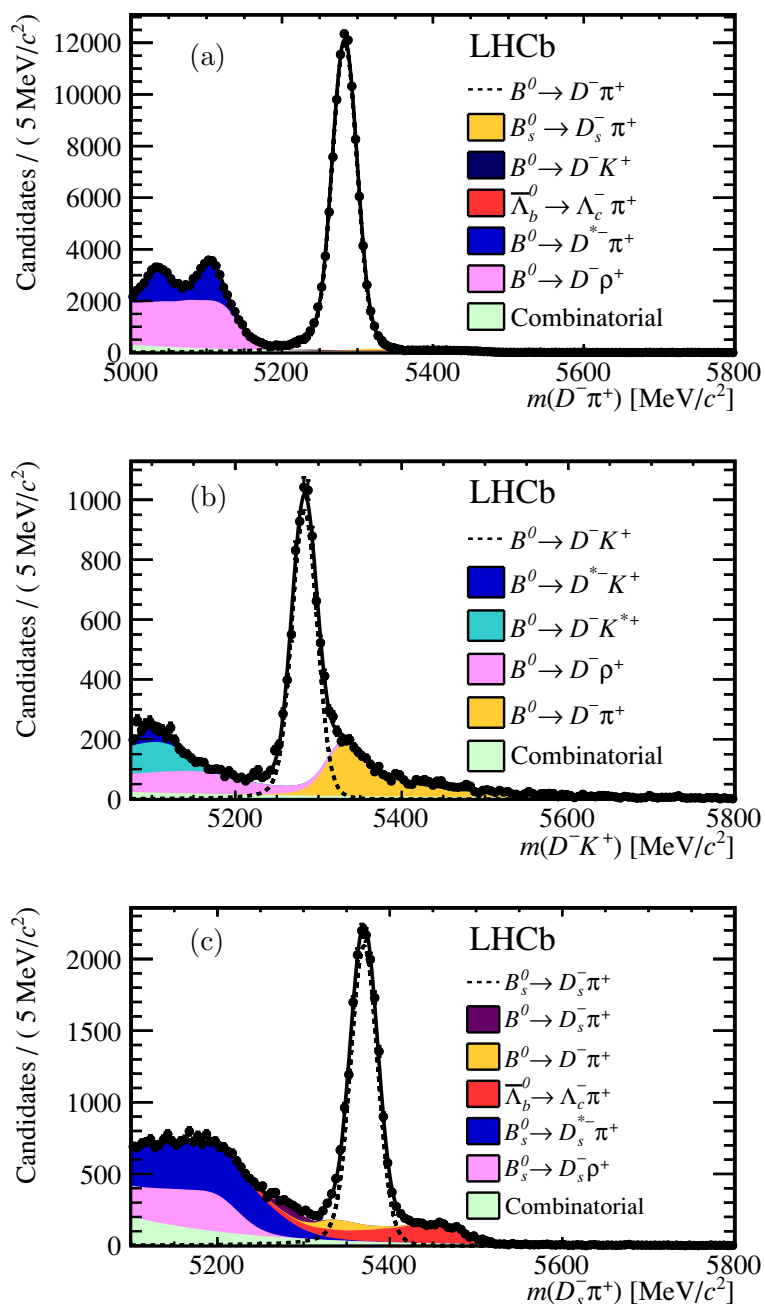
Figure 1. Invariant mass distributions of (a) $B^0 \to D^- \pi^+$ (b) $B^0 \to D^- K^+$ and (c) $B_s^0 \to D_s^- \pi^+$ candidates. The solid line is the result of the fit and the dotted line indicates the signal. The stacked background shapes follow the same top-to-bottom order in the legend and the plot. The B_s^0 and $\overline{\Lambda}_b^0$ backgrounds in the $B^0 \to D^- \pi^+$ mass distribution are invisibly small. The resulting signal yields are listed in table 1. For illustration purposes the figures include events from both magnet polarities, although they are fitted separately as described in the text.

Signal	Yield
$B^0 \to D^- \pi^+$	$106\,197 \pm 344$
$B^0 \to D^- K^+$	$7\,664 \pm 99$
$B_s^0 \to D_s^- \pi^+$	$17\,419 \pm 155$

Table 1. Yields obtained from the fits to the invariant mass distributions.

The invariant mass distributions of the misidentified decays are affected by the PID criteria. The shapes are obtained from simulated events, with the appropriate mass hypothesis applied. The distribution is then reweighted in a data-driven way, according to the particle identification cut efficiency obtained from the calibration sample, which is strongly dependent on the momentum of the particle.

Despite the small $\pi \to K$ misidentification probability of 2.8%, the largest misidentified background in the $B^0 \to D^- K^+$ sample originates from Cabibbo-favoured $B^0 \to D^- \pi^+$ decays where the bachelor pion is misidentified as a kaon. The shape of this particular misidentified decay is determined from data using a high purity sample of $B^0 \to D^- \pi^+$ decays (see figure 1(a)), obtained by selecting events in a narrow mass window 5200–5340 MeV/c^2. The yield of this prominent peaking background is allowed to vary in the fit and is found to be consistent with the expected yield based on the $B^0 \to D^- \pi^+$ signal yield and the misidentification probability. The contamination of $B^0 \to D^- \pi^+$ events in the $B_s^0 \to D_s^- \pi^+$ sample can be caused by the misidentification of either pion from the D^- decay. The misidentification probability is 2.0% (3.2%) for the higher (lower) p_{T} pion. After selecting the D_s^- candidate within the mass window around the nominal D_s^- mass [2], the number of misidentified pions is reduced to 0.75% (0.02%). The yield of this background is constrained in the fit, based on the $B^0 \to D^- \pi^+$ signal yield, the misidentification probability and their associated uncertainties.

The yield of $\overline{\Lambda}_b^0 \to \Lambda_c^- \pi^+$ decays is allowed to vary in the fit. The cross-feeds from $B^0 \to D^- K^+$ and $B_s^0 \to D_s^- \pi^+$ events in the $B^0 \to D^- \pi^+$ signal is small, and are constrained to their respective predicted yields. In addition, a contribution from the rare $B^0 \to D_s^- \pi^+$ decay is expected with a yield of 3.3% compared to the $B_s^0 \to D_s^- \pi^+$ signal, and is accounted for accordingly.

The combinatorial background consists of events with random pions and kaons, forming a fake D^- or D_s^- candidate, as well as real D^- or D_s^- mesons, that combine with a random pion or kaon. The combinatorial background is modelled with an exponential shape.

The results of the fits are presented in figure 1, and the corresponding signal yields are listed in table 1. The total yields of the decays $B^0 \to D^- \pi^+$ and $B^0 \to D^- K^+$ are used to determine the ratio of their branching fractions, while the event yields of the decays $B_s^0 \to D_s^- \pi^+$ and $B^0 \to D^- K^+$ are used to measure the average ratio of fragmentation fractions.

The dependence of the relative b-hadron production fractions as a function of the transverse momentum and pseudorapidity of the $B^0_{(s)}$ meson is studied in the ranges $2.0 < \eta < 5.0$ and $1.5 < p_{\mathrm{T}} < 40$ GeV/c, using $B^0 \to D^- \pi^+$ and $B_s^0 \to D_s^- \pi^+$ decays. The

Source	$\frac{B^0 \to D^- \pi^+}{B^0 \to D^- K^+}$ (%)	$\frac{B^0_s \to D^-_s \pi^+}{B^0 \to D^- K^+}$ (%)	$\frac{B^0_s \to D^-_s \pi^+}{B^0 \to D^- \pi^+}$ (%)
Detector acceptance			
and reconstruction	0.7	0.7	2.0 − 2.9
Hardware trigger efficiency	2.0	2.0	0.8
Offline selection	1.2	1.1	1.2
BDT cut	1.0	1.0	1.5
PID selection	1.0	1.5	1.1
Comb. background	0.7	1.0	0.8
Signal shape (tails)	0.5	0.6	[correl.]
Signal shape (core)	0.8	1.0	[correl.]
Charmless background	0.4	—	[correl.]
Total	3.1	3.4	3.2 − 3.8

Table 2. Systematic uncertainties for the measurement of the corrected ratio of event yields used for the measurements of f_s/f_d and the relative branching fraction of $B^0 \to D^- K^+$. The systematic uncertainty in p_T and η bins is shown as a range in the last column, and the total systematic uncertainty is the quadratic sum of the uncorrelated uncertainties. The systematic uncertainties on the ratio of $B^0 \to D^- \pi^+$ and $B^0_s \to D^-_s \pi^+$ yields that are correlated among the bins do not affect the dependence on p_T or η, and are not accounted for in the total systematic uncertainty.

event sample is subdivided in 20 bins in p_T and 10 bins in η, with the bin sizes chosen to obtain approximately equal number of events per bin. The fitting model for each bin is the same as that for the integrated samples, apart from the treatment of the exponent of the combinatorial background distribution, which is fixed to the value obtained from the fits to the integrated sample.

5 Systematic uncertainties

The systematic uncertainties on the measurement of the relative event yields of the $B^0 \to D^- \pi^+$, $B^0 \to D^- K^+$ and $B^0_s \to D^-_s \pi^+$ decay modes are related to trigger and offline selection efficiency corrections, particle identification calibration and the fit model.

The response to charged pions and kaons of the hadronic calorimeter used at the hardware trigger level has been investigated. As the hardware trigger mostly triggers on the high-p_T bachelor, a systematic uncertainty of 2% is assigned to the ratio of trigger efficiencies for the decays $B^0 \to D^- K^+$ and $B^0 \to D^- \pi^+$, estimated from dedicated studies with $D^{*-} \to \overline{D}^0 (K^+ \pi^-) \pi^-$ decays. This uncertainty is assumed to be uncorrelated between the individual bins in the binned analysis.

The relative selection efficiencies from simulation are studied by varying the BDT criterion, changing the signal yields by about ±25%. The variation of the relative efficiency is 1.0% which is assigned as systematic uncertainty.

The uncertainty on the PID efficiencies is estimated by comparing, in simulated events, the results obtained using the D^{*-} calibration sample to the true simulated PID perfor-

mance on the signal decays. The corresponding uncertainty ranges from 1.0% to 1.5% for the different measurements.

The exponent of the combinatorial background distribution is allowed to vary in the fits to the $B^0 \to D^- \pi^+$ and $B_s^0 \to D_s^- \pi^+$ mass distributions. By studying $D^- \pi^-$ and $D^- K^-$ combinations, it is suggested that the value of the exponent is smaller for the $B^0 \to D^- K^+$ decays than for the $B^0 \to D^- \pi^+$ decays, and therefore in the fit to the $B^0 \to D^- K^+$ candidates the exponent is fixed to half the value found in the fit to the $B^0 \to D^- \pi^+$ sample. The uncertainty on the signal yields due to the shape of the combinatorial background is estimated by reducing the exponent to half its value in the fits to the $B^0 \to D^- \pi^+$ and $B_s^0 \to D_s^- \pi^+$ mass distributions, and by taking a flat background for the fit to the $B^0 \to D^- K^+$ mass distribution. An uncertainty of 1.0% (0.7%) is assigned to the relative $B^0 \to D^- K^+$ and $B_s^0 \to D_s^- \pi^+$ ($B^0 \to D^- \pi^+$) yields.

The tails of the signal distributions are fixed from simulation due to the presence of large amounts of partially reconstructed decays in the lower sidebands. The uncertainty on the signal yield is estimated by varying the parameters that describe the tails by 10%. The uncertainty from the shape of the central peak is taken from a fit allowing for two different widths for the Crystal Ball functions in eq. 4.1, leading to a 1.0% (0.8%) uncertainty on the relative $B^0 \to D^- K^+$ and $B_s^0 \to D_s^- \pi^+$ ($B^0 \to D^- \pi^+$) yields.

The contribution of *charmless* B decays without an intermediate D meson is ignored in the fit. To evaluate the systematic uncertainty due to these decays, the B mass spectra for candidates in the sidebands of the D mass distribution are examined. A contribution of 0.4% relative to the signal yield is found in the $B^0 \to D^- \pi^+$ decay mode, and no contribution is seen in the other modes. For the $B^0 \to D^- \pi^+$ decay mode no correction is applied and the full size is taken as an uncertainty. No systematic uncertainty is assigned for the other decay modes.

The various sources of the systematic uncertainty that contribute to the uncertainties on the ratios of signal yields are listed in table 2. No uncertainty is associated to the $\overline{\Lambda}_b^0 \to \Lambda_c^- \pi^+$ background, as the yield is allowed to vary in the fit. Other cross checks, like varying the $B^0 \to D_s^- \pi^+$ yield in the $B_s^0 \to D_s^- \pi^+$ fit or including $\overline{\Lambda}_b^0 \to \Lambda_c^- K^+$ in the $B^0 \to D^- K^+$ fit, show a negligible effect on the signal yields.

All systematic variations are also performed in bins, and the corresponding relative changes in the ratio of yields have been quantified. Variations showing correlated behaviour do not affect the slope and are therefore not considered further.

6 Results

The relative signal yields of the decays $B^0 \to D^- \pi^+$, $B^0 \to D^- K^+$ and $B_s^0 \to D_s^- \pi^+$ are used to determine the branching fraction of the decay $B^0 \to D^- K^+$, and the ratio of fragmentation fractions f_s/f_d .

The efficiency corrected ratio of $B^0 \to D^- K^+$ and $B^0 \to D^- \pi^+$ signal yields results in the ratio of branching fractions

$$\frac{\mathcal{B}\left(B^0 \to D^- K^+\right)}{\mathcal{B}\left(B^0 \to D^- \pi^+\right)} = 0.0822 \pm 0.0011\,(\text{stat}) \pm 0.0025\,(\text{syst}).$$
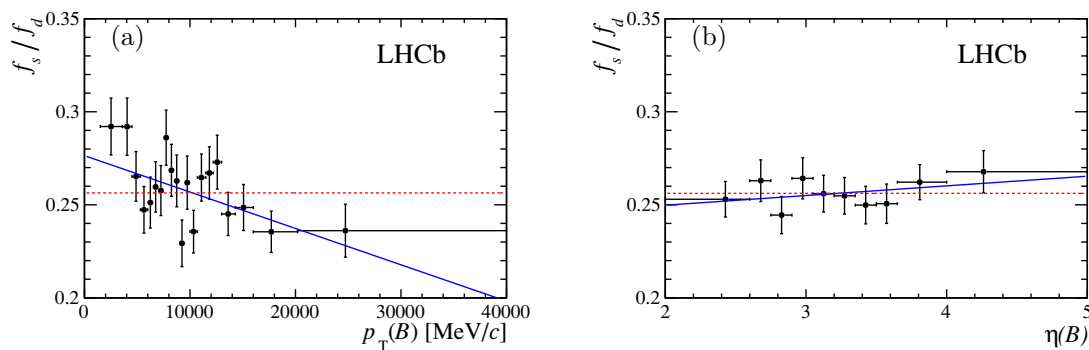
Figure 2. Ratio of fragmentation fractions f_s/f_d as functions of (a) $p_{\rm T}$ and (b) η. The errors on the data points are the statistical and uncorrelated systematic uncertainties added in quadrature. The solid line is the result of a linear fit, and the dashed line corresponds to the fit for the no-dependence hypothesis. The average value of $p_{\rm T}$ or η is determined for each bin and used as the center of the bin. The horizontal error bars indicate the bin size. Note that the scale is zero suppressed.

This is combined with the world average branching fraction $\mathcal{B}\left(B^0 \to D^- \pi^+\right) = (26.8 \pm 1.3) \times 10^{-4}$ [2], to give

$$\mathcal{B}\left(B^0 \to D^- K^+\right) = (2.20 \pm 0.03 \pm 0.07 \pm 0.11) \times 10^{-4},$$

where the first uncertainty is statistical, the second is systematic and the last is due to the uncertainty on the $B^0 \to D^- \pi^+$ branching fraction.

The ratio of fragmentation fractions is determined from the efficiency corrected event yields. The ratio of efficiencies is 0.913 ± 0.027. This results in

$$\frac{f_s}{f_d} = (0.261 \pm 0.004 \pm 0.017) \times \frac{1}{\mathcal{N}_a \mathcal{N}_F}$$

$$= 0.238 \pm 0.004 \pm 0.015 \pm 0.021,$$

where the first uncertainty is statistical, the second is systematic containing the sources listed in table 2 as well as errors from external measurements, and the third is theoretical, due to the knowledge of $\mathcal{N}_a$ and $\mathcal{N}_F$. The last source is dominated by the uncertainty on the form factor ratio.

This measurement supersedes and is in agreement with the previous determination with hadronic decays [3]. It also agrees with the previous measurement based on semileptonic decays [4]. The two independent results are combined taking into account the various sources of correlated systematic uncertainties, notably the $D_{(s)}^-$ branching fractions and $B_{(s)}^0$ lifetimes, to give

$$\frac{f_s}{f_d} = 0.256 \pm 0.020, \tag{6.1}$$

which supersedes the previous measurement from LHCb.

The value of f_s/f_d in bins of p_T or η is determined using the $B_s^0 \to D_s^- \pi^+$ and $B^0 \to D^- \pi^+$ decay modes and is presented in figure 2. A linear χ^2 fit gives

$$f_s/f_d \ (p_T) = (0.256 \pm 0.020) + (-2.0 \pm 0.6) \times 10^{-3}/\,\mathrm{GeV}/c \times (p_T - \langle p_T \rangle)$$
$$f_s/f_d \ (\eta) = (0.256 \pm 0.020) + (0.005 \pm 0.006) \times (\eta - \langle \eta \rangle),$$

with $\langle p_T \rangle = 10.4\,\mathrm{GeV}/c$ and $\langle \eta \rangle = 3.28$. The data points are normalised with a scale factor to match the average value of 0.256. The uncertainty associated to this parameter is taken from eq. 6.1, whilst the error from the fit is 0.003 for both p_T and η.

The p-value for this linear fit is found to be 0.16 (0.87) for p_T (η). The observed slope for the dependence on the transverse momentum of the $B_{(s)}^0$ meson deviates from zero with a significance of three standard deviations. No indication of a dependence on $\eta(B)$ is found.

7 Conclusions

The relative production rate of B_s^0 and B^0 mesons is determined using the hadronic decays $B_s^0 \to D_s^- \pi^+$ and $B^0 \to D^- K^+$ resulting in $f_s/f_d = 0.238 \pm 0.004\mathrm{(stat)} \pm 0.015\mathrm{(syst)} \pm 0.021\mathrm{(theo)}$. This value is consistent with a previous LHCb measurement based on semileptonic decays, with which it is averaged to obtain $f_s/f_d = 0.256 \pm 0.020$. The ratio of fragmentation fractions f_s/f_d is determined as a function of the transverse momentum and pseudorapidity of the $B_{(s)}^0$ meson, and a variation consistent with a linear dependence on the transverse momentum of the the $B_{(s)}^0$ meson is observed, with a significance of three standard deviations. In addition, the ratio of branching fractions of the decays $B^0 \to D^- K^+$ and $B^0 \to D^- \pi^+$ is measured to be $0.0822 \pm 0.0011\,\mathrm{(stat)} \pm 0.0025\,\mathrm{(syst)}$.

References

[1] LHCʙ collaboration, *First evidence for the decay* $B_s \to \mu^+\mu^-$, *Phys. Rev. Lett.* **110** (2013) 021801 [arXiv:1211.2674] [ɪɴSPIRE].

[2] Pᴀʀᴛɪᴄʟᴇ Dᴀᴛᴀ Gʀᴏᴜᴘ collaboration, J. Beringer et al., *Review of particle physics*, *Phys. Rev.* **D 86** (2012) 010001 [ɪɴSPIRE].

[3] LHCʙ collaboration, *Determination of* f_s/f_d *for* 7 TeV *pp collisions and a measurement of the branching fraction of the decay* $B_d \to D^- K^+$", *Phys. Rev. Lett.* **107** (2011) 211801 [arXiv:1106.4435] [ɪɴSPIRE].

[4] LHCʙ collaboration, *Measurement of b-hadron production fractions in* 7 TeVpp *collisions*, *Phys. Rev.* **D 85** (2012) 032008 [arXiv:1111.2357] [ɪɴSPIRE].

[5] M. Beneke, G. Buchalla, M. Neubert and C.T. Sachrajda, *QCD factorization for exclusive, nonleptonic B meson decays: General arguments and the case of heavy light final states*, *Nucl. Phys.* **B 591** (2000) 313 [hep-ph/0006124] [ɪɴSPIRE].

[6] R. Fleischer, N. Serra and N. Tuning, *A new strategy for* B_s *branching ratio measurements and the search for new physics in* $B_s^0 \to \mu^+\mu^-$, *Phys. Rev.* **D 82** (2010) 034038 [arXiv:1004.3982] [ɪɴSPIRE].

[7] Hᴇᴀᴠʏ Fʟᴀᴠᴏʀ Aᴠᴇʀᴀɢɪɴɢ Gʀᴏᴜᴘ collaboration, Y. Amhis et al., *Averages of b-hadron, c-hadron and* τ-*lepton properties as of early 2012*, arXiv:1207.1158 [ɪɴSPIRE].

[8] CLEO collaboration, S. Dobbs et al., *Measurement of absolute hadronic branching fractions of D mesons and* $e^+e^- \to D\bar{D}$ *cross-sections at the* $\psi(3770)$, *Phys. Rev.* **D 76** (2007) 112001 [arXiv:0709.3783] [ɪɴSPIRE].

[9] CLEO collaboration, J. Alexander et al., *Absolute measurement of hadronic branching fractions of the* D_s^+ *meson*, *Phys. Rev. Lett.* **100** (2008) 161804 [arXiv:0801.0680] [ɪɴSPIRE].

[10] R. Fleischer, N. Serra and N. Tuning, *Tests of Factorization and* SU(3) *Relations in B Decays into Heavy-Light Final States*, *Phys. Rev.* **D 83** (2011) 014017 [arXiv:1012.2784] [ɪɴSPIRE].

[11] J.A. Bailey et al., $B_s \to D_s/B \to D$ *semileptonic form-factor ratios and their application to* $BR(B_s^0 \to \mu^+\mu^-)$, *Phys. Rev.* **D 85** (2012) 114502 [*Erratum ibid.* **D 86** (2012) 039904] [arXiv:1202.6346] [ɪɴSPIRE].

[12] LHCb collaboration, *The LHCb detector at the LHC*, 2008 *JINST* **3** S08005 [ɪɴSPIRE].

[13] R. Aaij et al., *The LHCb trigger and its performance*, arXiv:1211.3055 [ɪɴSPIRE].

[14] T. Sjöstrand, S. Mrenna and P.Z. Skands, *PYTHIA 6.4 physics and manual*, *JHEP* **05** (2006) 026 [hep-ph/0603175] [ɪɴSPIRE].

[15] I. Belyaev et al., *Handling of the generation of primary events in* Gᴀᴜss, *the LHCb simulation framework*, *IEEE Nucl. Sci. Symp. Conf. Rec.* (2010) 1155.

[16] D. Lange, *The EvtGen particle decay simulation package*, *Nucl. Instrum. Meth.* **A 462** (2001) 152 [ɪɴSPIRE].

[17] P. Golonka and Z. Was, *PHOTOS Monte Carlo: a precision tool for QED corrections in Z and W decays*, *Eur. Phys. J.* **C 45** (2006) 97 [hep-ph/0506026] [ɪɴSPIRE].

[18] GEANT4 collaboration, J. Allison et al., *GEANT4 developments and applications*, *IEEE Trans. Nucl. Sci.* **53** (2006) 270.

[19] GEANT4 collaboration, S. Agostinelli et al., *GEANT4: a simulation toolkit*, *Nucl. Instrum. Meth.* **A 506** (2003) 250 [inSPIRE].

[20] M. Clemencic et al., *The LHCb simulation application*, Gauss: *design, evolution and experience*, *J. Phys. Conf. Ser.* **331** (2011) 032023.

[21] L. Breiman, J.H. Friedman, R.A. Olshen and C.J. Stone, *Classification and regression trees*, Wadsworth international group, Belmont U.S.A. (1984).

[22] BABAR collaboration, P. del Amo Sanchez et al., *Dalitz plot analysis of $D_s^+ \to K^+ K^- \pi^+$*, *Phys. Rev.* **D 83** (2011) 052001 [arXiv:1011.4190] [inSPIRE].

[23] CLEO collaboration, G. Bonvicini et al., *Dalitz plot analysis of the $D^+ \to K^- \pi^+ \pi^+$ decay*, *Phys. Rev.* **D 78** (2008) 052001 [arXiv:0802.4214] [inSPIRE].

[24] T. Skwarnicki, *A study of the radiative cascade transitions between the Υ' and Υ resonances*, Ph.D. thesis, Institute of Nuclear Physics, Krakow, Poland (1986) [inSPIRE].

The LHCb collaboration

R. Aaij[38], C. Abellan Beteta[33,n], A. Adametz[11], B. Adeva[34], M. Adinolfi[43], C. Adrover[6],
A. Affolder[49], Z. Ajaltouni[5], J. Albrecht[35], F. Alessio[35], M. Alexander[48], S. Ali[38], G. Alkhazov[27],
P. Alvarez Cartelle[34], A.A. Alves Jr[22,35], S. Amato[2], Y. Amhis[7], L. Anderlini[17,f], J. Anderson[37],
R. Andreassen[57], R.B. Appleby[51], O. Aquines Gutierrez[10], F. Archilli[18], A. Artamonov [32],
M. Artuso[53], E. Aslanides[6], G. Auriemma[22,m], S. Bachmann[11], J.J. Back[45], C. Baesso[54],
V. Balagura[28], W. Baldini[16], R.J. Barlow[51], C. Barschel[35], S. Barsuk[7], W. Barter[44], A. Bates[48],
Th. Bauer[38], A. Bay[36], J. Beddow[48], I. Bediaga[1], S. Belogurov[28], K. Belous[32], I. Belyaev[28],
E. Ben-Haim[8], M. Benayoun[8], G. Bencivenni[18], S. Benson[47], J. Benton[43], A. Berezhnoy[29],
R. Bernet[37], M.-O. Bettler[44], M. van Beuzekom[38], A. Bien[11], S. Bifani[12], T. Bird[51],
A. Bizzeti[17,h], P.M. Bjørnstad[51], T. Blake[35], F. Blanc[36], C. Blanks[50], J. Blouw[11], S. Blusk[53],
A. Bobrov[31], V. Bocci[22], A. Bondar[31], N. Bondar[27], W. Bonivento[15], S. Borghi[51], A. Borgia[53],
T.J.V. Bowcock[49], E. Bowen[37], C. Bozzi[16], T. Brambach[9], J. van den Brand[39], J. Bressieux[36],
D. Brett[51], M. Britsch[10], T. Britton[53], N.H. Brook[43], H. Brown[49], A. Büchler-Germann[37],
I. Burducea[26], A. Bursche[37], J. Buytaert[35], S. Cadeddu[15], O. Callot[7], M. Calvi[20,j],
M. Calvo Gomez[33,n], A. Camboni[33], P. Campana[18,35], A. Carbone[14,c], G. Carboni[21,k],
R. Cardinale[19,i], A. Cardini[15], H. Carranza-Mejia[47], L. Carson[50], K. Carvalho Akiba[2], G. Casse[49],
M. Cattaneo[35], Ch. Cauet[9], M. Charles[52], Ph. Charpentier[35], P. Chen[3,36], N. Chiapolini[37],
M. Chrzaszcz [23], K. Ciba[35], X. Cid Vidal[34], G. Ciezarek[50], P.E.L. Clarke[47], M. Clemencic[35],
H.V. Cliff[44], J. Closier[35], C. Coca[26], V. Coco[38], J. Cogan[6], E. Cogneras[5], P. Collins[35],
A. Comerma-Montells[33], A. Contu[15], A. Cook[43], M. Coombes[43], G. Corti[35], B. Couturier[35],
G.A. Cowan[36], D. Craik[45], S. Cunliffe[50], R. Currie[47], C. D'Ambrosio[35], P. David[8],
P.N.Y. David[38], I. De Bonis[4], K. De Bruyn[38], S. De Capua[51], M. De Cian[37], J.M. De Miranda[1],
L. De Paula[2], W. De Silva[57], P. De Simone[18], D. Decamp[4], M. Deckenhoff[9], H. Degaudenzi[36,35],
L. Del Buono[8], C. Deplano[15], D. Derkach[14], O. Deschamps[5], F. Dettori[39], A. Di Canto[11],
J. Dickens[44], H. Dijkstra[35], P. Diniz Batista[1], M. Dogaru[26], F. Domingo Bonal[33,n], S. Donleavy[49],
F. Dordei[11], A. Dosil Suárez[34], D. Dossett[45], A. Dovbnya[40], F. Dupertuis[36], R. Dzhelyadin[32],
A. Dziurda[23], A. Dzyuba[27], S. Easo[46,35], U. Egede[50], V. Egorychev[28], S. Eidelman[31],
D. van Eijk[38], S. Eisenhardt[47], U. Eitschberger[9], R. Ekelhof[9], L. Eklund[48], I. El Rifai[5],
Ch. Elsasser[37], D. Elsby[42], A. Falabella[14,e], C. Färber[11], G. Fardell[47], C. Farinelli[38], S. Farry[12],
V. Fave[36], D. Ferguson[47], V. Fernandez Albor[34], F. Ferreira Rodrigues[1], M. Ferro-Luzzi[35],
S. Filippov[30], C. Fitzpatrick[35], M. Fontana[10], F. Fontanelli[19,i], R. Forty[35], O. Francisco[2],
M. Frank[35], C. Frei[35], M. Frosini[17,f], S. Furcas[20], E. Furfaro[21], A. Gallas Torreira[34], D. Galli[14,c],
M. Gandelman[2], P. Gandini[52], Y. Gao[3], J. Garofoli[53], P. Garosi[51], J. Garra Tico[44], L. Garrido[33],
C. Gaspar[35], R. Gauld[52], E. Gersabeck[11], M. Gersabeck[51], T. Gershon[45,35], Ph. Ghez[4],
V. Gibson[44], V.V. Gligorov[35], C. Göbel[54], D. Golubkov[28], A. Golutvin[50,28,35], A. Gomes[2],
H. Gordon[52], M. Grabalosa Gándara[5], R. Graciani Diaz[33], L.A. Granado Cardoso[35],
E. Graugés[33], G. Graziani[17], A. Grecu[26], E. Greening[52], S. Gregson[44], O. Grünberg[55], B. Gui[53],
E. Gushchin[30], Yu. Guz[32], T. Gys[35], C. Hadjivasiliou[53], G. Haefeli[36], C. Haen[35], S.C. Haines[44],
S. Hall[50], T. Hampson[43], S. Hansmann-Menzemer[11], N. Harnew[52], S.T. Harnew[43], J. Harrison[51],
P.F. Harrison[45], T. Hartmann[55], J. He[7], V. Heijne[38], K. Hennessy[49], P. Henrard[5],
J.A. Hernando Morata[34], E. van Herwijnen[35], E. Hicks[49], D. Hill[52], M. Hoballah[5], C. Hombach[51],
P. Hopchev[4], W. Hulsbergen[38], P. Hunt[52], T. Huse[49], N. Hussain[52], D. Hutchcroft[49], D. Hynds[48],
V. Iakovenko[41], P. Ilten[12], J. Imong[43], R. Jacobsson[35], A. Jaeger[11], E. Jans[38], F. Jansen[38],
P. Jaton[36], F. Jing[3], M. John[52], D. Johnson[52], C.R. Jones[44], B. Jost[35], M. Kaballo[9],
S. Kandybei[40], M. Karacson[35], T.M. Karbach[35], I.R. Kenyon[42], U. Kerzel[35], T. Ketel[39],
A. Keune[36], B. Khanji[20], O. Kochebina[7], I. Komarov[36,29], R.F. Koopman[39], P. Koppenburg[38],

M. Korolev[29], A. Kozlinskiy[38], L. Kravchuk[30], K. Kreplin[11], M. Kreps[45], G. Krocker[11],
P. Krokovny[31], F. Kruse[9], M. Kucharczyk[20,23,j], V. Kudryavtsev[31], T. Kvaratskheliya[28,35],
V.N. La Thi[36], D. Lacarrere[35], G. Lafferty[51], A. Lai[15], D. Lambert[47], R.W. Lambert[39],
E. Lanciotti[35], G. Lanfranchi[18,35], C. Langenbruch[35], T. Latham[45], C. Lazzeroni[42], R. Le Gac[6],
J. van Leerdam[38], J.-P. Lees[4], R. Lefèvre[5], A. Leflat[29,35], J. Lefrançois[7], O. Leroy[6], Y. Li[3],
L. Li Gioi[5], M. Liles[49], R. Lindner[35], C. Linn[11], B. Liu[3], G. Liu[35], J. von Loeben[20], J.H. Lopes[2],
E. Lopez Asamar[33], N. Lopez-March[36], H. Lu[3], J. Luisier[36], H. Luo[47], A. Mac Raighne[48],
F. Machefert[7], I.V. Machikhiliyan[4,28], F. Maciuc[26], O. Maev[27,35], S. Malde[52], G. Manca[15,d],
G. Mancinelli[6], N. Mangiafave[44], U. Marconi[14], R. Märki[36], J. Marks[11], G. Martellotti[22],
A. Martens[8], L. Martin[52], A. Martín Sánchez[7], M. Martinelli[38], D. Martinez Santos[39],
D. Martins Tostes[2], A. Massafferri[1], R. Matev[35], Z. Mathe[35], C. Matteuzzi[20], M. Matveev[27],
E. Maurice[6], A. Mazurov[16,30,35,e], J. McCarthy[42], R. McNulty[12], B. Meadows[57,52], F. Meier[9],
M. Meissner[11], M. Merk[38], D.A. Milanes[13], M.-N. Minard[4], J. Molina Rodriguez[54], S. Monteil[5],
D. Moran[51], P. Morawski[23], R. Mountain[53], I. Mous[38], F. Muheim[47], K. Müller[37], R. Muresan[26],
B. Muryn[24], B. Muster[36], P. Naik[43], T. Nakada[36], R. Nandakumar[46], I. Nasteva[1], M. Needham[47],
N. Neufeld[35], A.D. Nguyen[36], T.D. Nguyen[36], C. Nguyen-Mau[36,o], M. Nicol[7], V. Niess[5], R. Niet[9],
N. Nikitin[29], T. Nikodem[11], S. Nisar[56], A. Nomerotski[52], A. Novoselov[32],
A. Oblakowska-Mucha[24], V. Obraztsov[32], S. Oggero[38], S. Ogilvy[48], O. Okhrimenko[41],
R. Oldeman[15,d,35], M. Orlandea[26], J.M. Otalora Goicochea[2], P. Owen[50], B.K. Pal[53],
A. Palano[13,b], M. Palutan[18], J. Panman[35], A. Papanestis[46], M. Pappagallo[48], C. Parkes[51],
C.J. Parkinson[50], G. Passaleva[17], G.D. Patel[49], M. Patel[50], G.N. Patrick[46], C. Patrignani[19,i],
C. Pavel-Nicorescu[26], A. Pazos Alvarez[34], A. Pellegrino[38], G. Penso[22,l], M. Pepe Altarelli[35],
S. Perazzini[14,c], D.L. Perego[20,j], E. Perez Trigo[34], A. Pérez-Calero Yzquierdo[33], P. Perret[5],
M. Perrin-Terrin[6], G. Pessina[20], K. Petridis[50], A. Petrolini[19,i], A. Phan[53], E. Picatoste Olloqui[33],
B. Pietrzyk[4], T. Pilař[45], D. Pinci[22], S. Playfer[47], M. Plo Casasus[34], F. Polci[8], G. Polok[23],
A. Poluektov[45,31], E. Polycarpo[2], D. Popov[10], B. Popovici[26], C. Potterat[33], A. Powell[52],
J. Prisciandaro[36], V. Pugatch[41], A. Puig Navarro[36], W. Qian[4], J.H. Rademacker[43],
B. Rakotomiaramanana[36], M.S. Rangel[2], I. Raniuk[40], N. Rauschmayr[35], G. Raven[39],
S. Redford[52], M.M. Reid[45], A.C. dos Reis[1], S. Ricciardi[46], A. Richards[50], K. Rinnert[49],
V. Rives Molina[33], D.A. Roa Romero[5], P. Robbe[7], E. Rodrigues[51], P. Rodriguez Perez[34],
G.J. Rogers[44], S. Roiser[35], V. Romanovsky[32], A. Romero Vidal[34], J. Rouvinet[36], T. Ruf[35],
H. Ruiz[33], G. Sabatino[22,k], J.J. Saborido Silva[34], N. Sagidova[27], P. Sail[48], B. Saitta[15,d],
C. Salzmann[37], B. Sanmartin Sedes[34], M. Sannino[19,i], R. Santacesaria[22], C. Santamarina Rios[34],
E. Santovetti[21,k], M. Sapunov[6], A. Sarti[18,l], C. Satriano[22,m], A. Satta[21], M. Savrie[16,e],
D. Savrina[28,29], P. Schaack[50], M. Schiller[39], H. Schindler[35], S. Schleich[9], M. Schlupp[9],
M. Schmelling[10], B. Schmidt[35], O. Schneider[36], A. Schopper[35], M.-H. Schune[7], R. Schwemmer[35],
B. Sciascia[18], A. Sciubba[18,l], M. Seco[34], A. Semennikov[28], K. Senderowska[24], I. Sepp[50],
N. Serra[37], J. Serrano[6], P. Seyfert[11], M. Shapkin[32], I. Shapoval[40,35], P. Shatalov[28],
Y. Shcheglov[27], T. Shears[49,35], L. Shekhtman[31], O. Shevchenko[40], V. Shevchenko[28], A. Shires[50],
R. Silva Coutinho[45], T. Skwarnicki[53], N.A. Smith[49], E. Smith[52,46], M. Smith[51], K. Sobczak[5],
M.D. Sokoloff[57], F.J.P. Soler[48], F. Soomro[18,35], D. Souza[43], B. Souza De Paula[2], B. Spaan[9],
A. Sparkes[47], P. Spradlin[48], F. Stagni[35], S. Stahl[11], O. Steinkamp[37], S. Stoica[26], S. Stone[53],
B. Storaci[37], M. Straticiuc[26], U. Straumann[37], V.K. Subbiah[35], S. Swientek[9], V. Syropoulos[39],
M. Szczekowski[25], P. Szczypka[36,35], T. Szumlak[24], S. T'Jampens[4], M. Teklishyn[7],
E. Teodorescu[26], F. Teubert[35], C. Thomas[52], E. Thomas[35], J. van Tilburg[11], V. Tisserand[4],
M. Tobin[37], S. Tolk[39], D. Tonelli[35], S. Topp-Joergensen[52], N. Torr[52], E. Tournefier[4,50],
S. Tourneur[36], M.T. Tran[36], M. Tresch[37], A. Tsaregorodtsev[6], P. Tsopelas[38], N. Tuning[38],
M. Ubeda Garcia[35], A. Ukleja[25], D. Urner[51], U. Uwer[11], V. Vagnoni[14], G. Valenti[14],

R. Vazquez Gomez[33], P. Vazquez Regueiro[34], S. Vecchi[16], J.J. Velthuis[43], M. Veltri[17,g],
G. Veneziano[36], M. Vesterinen[35], B. Viaud[7], D. Vieira[2], X. Vilasis-Cardona[33,n], A. Vollhardt[37],
D. Volyanskyy[10], D. Voong[43], A. Vorobyev[27], V. Vorobyev[31], C. Voß[55], H. Voss[10], R. Waldi[55],
R. Wallace[12], S. Wandernoth[11], J. Wang[53], D.R. Ward[44], N.K. Watson[42], A.D. Webber[51],
D. Websdale[50], M. Whitehead[45], J. Wicht[35], D. Wiedner[11], L. Wiggers[38], G. Wilkinson[52],
M.P. Williams[45,46], M. Williams[50,p], F.F. Wilson[46], J. Wishahi[9], M. Witek[23], W. Witzeling[35],
S.A. Wotton[44], S. Wright[44], S. Wu[3], K. Wyllie[35], Y. Xie[47,35], F. Xing[52], Z. Xing[53], Z. Yang[3],
R. Young[47], X. Yuan[3], O. Yushchenko[32], M. Zangoli[14], M. Zavertyaev[10,a], F. Zhang[3], L. Zhang[53],
W.C. Zhang[12], Y. Zhang[3], A. Zhelezov[11], A. Zhokhov[28], L. Zhong[3], A. Zvyagin[35]

1 Centro Brasileiro de Pesquisas Físicas (CBPF), Rio de Janeiro, Brazil
2 Universidade Federal do Rio de Janeiro (UFRJ), Rio de Janeiro, Brazil
3 Center for High Energy Physics, Tsinghua University, Beijing, China
4 LAPP, Université de Savoie, CNRS/IN2P3, Annecy-Le-Vieux, France
5 Clermont Université, Université Blaise Pascal, CNRS/IN2P3, LPC, Clermont-Ferrand, France
6 CPPM, Aix-Marseille Université, CNRS/IN2P3, Marseille, France
7 LAL, Université Paris-Sud, CNRS/IN2P3, Orsay, France
8 LPNHE, Université Pierre et Marie Curie, Université Paris Diderot, CNRS/IN2P3, Paris, France
9 Fakultät Physik, Technische Universität Dortmund, Dortmund, Germany
10 Max-Planck-Institut für Kernphysik (MPIK), Heidelberg, Germany
11 Physikalisches Institut, Ruprecht-Karls-Universität Heidelberg, Heidelberg, Germany
12 School of Physics, University College Dublin, Dublin, Ireland
13 Sezione INFN di Bari, Bari, Italy
14 Sezione INFN di Bologna, Bologna, Italy
15 Sezione INFN di Cagliari, Cagliari, Italy
16 Sezione INFN di Ferrara, Ferrara, Italy
17 Sezione INFN di Firenze, Firenze, Italy
18 Laboratori Nazionali dell'INFN di Frascati, Frascati, Italy
19 Sezione INFN di Genova, Genova, Italy
20 Sezione INFN di Milano Bicocca, Milano, Italy
21 Sezione INFN di Roma Tor Vergata, Roma, Italy
22 Sezione INFN di Roma La Sapienza, Roma, Italy
23 Henryk Niewodniczanski Institute of Nuclear Physics Polish Academy of Sciences, Kraków, Poland
24 AGH University of Science and Technology, Kraków, Poland
25 National Center for Nuclear Research (NCBJ), Warsaw, Poland
26 Horia Hulubei National Institute of Physics and Nuclear Engineering, Bucharest-Magurele, Romania
27 Petersburg Nuclear Physics Institute (PNPI), Gatchina, Russia
28 Institute of Theoretical and Experimental Physics (ITEP), Moscow, Russia
29 Institute of Nuclear Physics, Moscow State University (SINP MSU), Moscow, Russia
30 Institute for Nuclear Research of the Russian Academy of Sciences (INR RAN), Moscow, Russia
31 Budker Institute of Nuclear Physics (SB RAS) and Novosibirsk State University, Novosibirsk, Russia
32 Institute for High Energy Physics (IHEP), Protvino, Russia
33 Universitat de Barcelona, Barcelona, Spain
34 Universidad de Santiago de Compostela, Santiago de Compostela, Spain
35 European Organization for Nuclear Research (CERN), Geneva, Switzerland
36 Ecole Polytechnique Fédérale de Lausanne (EPFL), Lausanne, Switzerland
37 Physik-Institut, Universität Zürich, Zürich, Switzerland
38 Nikhef National Institute for Subatomic Physics, Amsterdam, The Netherlands
39 Nikhef National Institute for Subatomic Physics and VU University Amsterdam, Amsterdam, The Netherlands

40 *NSC Kharkiv Institute of Physics and Technology (NSC KIPT), Kharkiv, Ukraine*

41 *Institute for Nuclear Research of the National Academy of Sciences (KINR), Kyiv, Ukraine*

42 *University of Birmingham, Birmingham, United Kingdom*

43 *H.H. Wills Physics Laboratory, University of Bristol, Bristol, United Kingdom*

44 *Cavendish Laboratory, University of Cambridge, Cambridge, United Kingdom*

45 *Department of Physics, University of Warwick, Coventry, United Kingdom*

46 *STFC Rutherford Appleton Laboratory, Didcot, United Kingdom*

47 *School of Physics and Astronomy, University of Edinburgh, Edinburgh, United Kingdom*

48 *School of Physics and Astronomy, University of Glasgow, Glasgow, United Kingdom*

49 *Oliver Lodge Laboratory, University of Liverpool, Liverpool, United Kingdom*

50 *Imperial College London, London, United Kingdom*

51 *School of Physics and Astronomy, University of Manchester, Manchester, United Kingdom*

52 *Department of Physics, University of Oxford, Oxford, United Kingdom*

53 *Syracuse University, Syracuse, NY, United States*

54 *Pontifícia Universidade Católica do Rio de Janeiro (PUC-Rio), Rio de Janeiro, Brazil, associated to[2]*

55 *Institut für Physik, Universität Rostock, Rostock, Germany, associated to[11]*

56 *Institute of Information Technology, COMSATS, Lahore, Pakistan, associated to[53]*

57 *University of Cincinnati, Cincinnati, OH, United States, associated to[53]*

[a] *P.N. Lebedev Physical Institute, Russian Academy of Science (LPI RAS), Moscow, Russia*

[b] *Università di Bari, Bari, Italy*

[c] *Università di Bologna, Bologna, Italy*

[d] *Università di Cagliari, Cagliari, Italy*

[e] *Università di Ferrara, Ferrara, Italy*

[f] *Università di Firenze, Firenze, Italy*

[g] *Università di Urbino, Urbino, Italy*

[h] *Università di Modena e Reggio Emilia, Modena, Italy*

[i] *Università di Genova, Genova, Italy*

[j] *Università di Milano Bicocca, Milano, Italy*

[k] *Università di Roma Tor Vergata, Roma, Italy*

[l] *Università di Roma La Sapienza, Roma, Italy*

[m] *Università della Basilicata, Potenza, Italy*

[n] *LIFAELS, La Salle, Universitat Ramon Llull, Barcelona, Spain*

[o] *Hanoi University of Science, Hanoi, Viet Nam*

[p] *Massachusetts Institute of Technology, Cambridge, MA, United States*